Supplemental Methods

Sequencing

Genomic DNA was extracted from adrenal tissue samples manually using the high salt method. *ARMC5*, *PRKAR1A* and *PRKACA* genes were sequenced by targeted next generation sequencing, using a set of primers designed using the AmpliSeq Designer (Life technologies) and amplyfing 91 amplicons. The library was generated using the Ion AmpliSeq Library Kit 2.0 (Life Technologies. Emulsion PCR was performed using the Ion OneTouch™ Instrument (Life Technologies). Enrichment of the template-positive Ion OneTouch™ 200 ion sphere™ particles (ISPs, containing clonally amplified DNA) PCR was performed using the Ion OneTouch™ ES (Life Technologies), were loaded on Ion 316™ chips and sequenced with an Ion Personal Genome Machine® (PGM™) System (Life Technologies). Data collected on the PGM were collated and reanalysed using the Torrent Suite 4.2 using FASTQ files from the Ion Torrent Browser. Sequence alignment and extraction of SNPs and short insertions/deletions (indels) were performed using the Variant Caller plugin. Of the Torrent Suite and The NextGENe software v2.3.3 (Softgenetics, State College, Pennsylvania, USA). *CTNNB1* gene (exon 3) and *GNAS* gene (exon 7-9) was sequenced by conventional Sanger sequencing. Sequencing products were analyzed with an automated capillary sequencer (ABI PRISM 3730S Genetic Analyzer; Applied Biosystems, Foster City, CA).

Gene expression studies

Gene expression analysis by RT-qPCR was performed in the 16 adrenal lesions, as well as in the adjacent non-tumorous adrenal tissue of patient #1, and 4 samples of unaffected adrenal tissue from 4 patients who underwent radical nephrectomy for renal cell carcinoma. Tissues were stored at –150° C until mRNA extraction with Trizol (Life Technologies, Saint Aubin, France) according to the manufacturer's recommendations. cDNA was obtained by reverse transcription of 1 µg of total RNA. Quantitative RT-PCR was performed using the Fast SYBR® Green Master Mix (Life Technologies) on a StepOnePlus™ Real-Time PCR system (Life Technologies).

Standard curves were generated by use of serial dilutions of linearized standard plasmids, spanning 6 orders of magnitude and yielding correlation coefficients larger than 0.98 and efficiencies of at least 0.95, in all experiments. The internal control gene for data normalization was *β-ACTIN*. The relative expression of each gene is expressed as the ratio of attomoles of the specific gene to attomoles of *β-ACTIN*. The primers for *ADRB1*, *AGTR1*, *AVPR1A*, *β-ACTIN*, *GIPR*, *GnRHR, HTR4, LHCGR, MC2R, QPCTL, SIX5, SNRPD2, FBXO46* and *ZMYND8* are shown in the Supplemental Table S4.

Oligonucleotide based array-comparative genomic hybridization analysis (array-CGH)

Genomic imbalances were analyzed by array-CGH using 400K oligonucleotide arrays (Agilent Technologies, Massy, France). DNA from adrenal samples was compared to blood donor genomic DNA. Hybridization was performed according to the manufacturer's protocol. Images were processed with Feature Extraction software (10.7.3.1) and data analysis was performed with Genomic Workbench V5.0.14 (Agilent Technologies). The genomic positions were determined using version 19 of the Human Genome (http://genome.ucsc.edu/). The ADM2 algorithm was used for statistical analysis. Copy number variations were considered significant if they were defined by four or more oligonucleotides and spanned at least 20 Kb (for 400K arrays, respectively) and were not identified in the Database of Genomic Variants (http://projects.tcag.ca/cgi-bin/variation/gbrowse/hg19).

RNA FISH and DNA FISH

For DNA FISH and for nascent transcript detection by RNA, the following BAC/Fosmid (CHORI) probes were used: GIPR/QPCTL/FBX046 locus (WI2-2971P5; only DNA FISH), GIPR (WI2-606G4; only RNA FISH) and ZMYND8 (RP4-569M23). The correct chromosomal location of BACs was first verified by DNA FISH on metaphase spreads. Probes were labeled by nick translation (Vysis) with Spectrum Red-dUTP, Spectrum Green-dUTP, or Cy5- dUTP following the manufacturer's instructions. DNA and RNA FISH were performed as previously described [1]. Samples proper quality for RNA and DNA FISH experiment was done using known working BAC-based probes routinely used in the laboratory.

Pyrosequencing

For pyrosequencing, 600 ng of genomic DNA were converted by bisulfite (Zymo Research, USA). The GIPR prompter region was first amplified by PCR and then pyrosequenced using PyroMark Q96 (Qiagen, Germany). The primers for the PCR and the pyrosequencing are given in the Supplemental Figure S3.

Mate-pair analysis and sequencing

Libraries were prepared from selected adrenal lesion's DNA, using the Nextera Mate-pair Sample Preparation Kit (Illumina, CA). Libraries were sequenced on a HiSeq2500, each yielding around 90 million pairs of 100-nucleotide-long reads. Sequencing data were processed as previously described [2] and treated reads were mapped on version hg19 of the Human Genome with Bfast and BWA 0.7.0a. BAM preprocessing and detection of abnormally mapped pairs were performed using SVDetect [3]. A minimum of 5 abnormally mapped pairs in a cluster was set as a threshold to detect a structural variation. Bioinformatics analysis was performed at nebula.curie.fr [4] and replicated with the Galaxy instance of Bicêtre hospital.

Plasmid constructs

A 1 kb fragment of the intron 2 region of the human *ZMYND8* gene, in which *SacI* and *XhoI* restriction sites were introduced to facilitate cloning into the pGL4.26-Luciferase vector (Promega, Charbonnières-Les-Bains, France), was amplified by PCR from genomic DNA by using the High-Fidelity Phusion DNA polymerase (Life Technologies) and specific primers (Supplemental Table S1), yielding the *ZMYND8* intron 2-pGL4.26-Luc plasmid construct (Supplemental Figure S2A). Luciferase cDNA with the minimal promoter was then removed from the plasmid construct after *HindIII* and *FseI* digestion. In parallel, the *GIPR* coding sequence was isolated from the hGIPR plasmid after *HindIII* and *XhoI* digestion. Both fragments were incubated with the Klenow fragment of DNA Polymerase I (New England Biolabs, Evry, France) to fill in 5' overhangs and form blunt ends. *GIPR* cDNA was then inserted

downstream of the human *ZMYND8* intron 2 region to obtain the *ZMYND8* intron 2-GIPR plasmid construct (Supplemental Figure S2B).

Luciferase reporter gene assays

HEK 293T cells were seeded 72 h before transfection at 6,000 cells/well in 96-well plates in high glucose DMEM medium containing 2 mM glutamine, 100 IU/mL penicillin, 100 µg/mL streptomycin, and 10% fetal calf serum (Biowest) at 37°C. Cell culture reagents were from Life Technologies excepted when stated. Cells were then cotransfected in serum-free OptiMEM® medium using the Lipofectamine® 2000 reagent according to the manufacturer's recommendations (Life Technologies), together with the *ZMYND8* intron 2-pGL4.26-Luc plasmid construct (40 ng), the human glucocorticoid receptor (hGR, 40 ng), pcDNA3.1 (20 ng) and the pMIR-Report™ β-gal control (35 ng) plasmids (Life Technologies), as an internal reporter plasmid control. Six hours after transfection, the culture medium was replaced by minimal medium containing 10% dextran charcoal-coated serum. The next day, cells were treated with 10^{-7} M dexamethasone (DEX) in minimal medium and cotreated with a glucocorticoid antagonist RU486 (10^{-5} M). Twenty-four hours later, cells were lysed in passive lysis buffer (Promega). Luciferase and β-galactosidase activities were expressed as a percentage of relative transcriptional activities compared with controls. The *ZMYND8* intron 2-GIPR plasmid construct (40 ng) was transfected, as described above, into HEK 293T cells, together with the hGR plasmid (40 ng), CRE-Luc (40 ng, Promega) and the pMIR-Report™ β-gal (35 ng) control plasmids. The day after transfection, cells were pre-treated with 10^{-7} M DEX in minimal medium in presence of 10^{-4} M Ro 20-1724 (Sigma Aldrich), a phosphodiesterase inhibitor, to induce maximal GIPR expression. Twenty-four hours later, cells were treated for 4 h in serum-free medium with ethanol, 10^{-7} M GIP, 10^{-5} M H-89, 10^{-7} M DEX or 10^{-5} M RU486. Luciferase activity normalized to β-galactosidase activity was determined as described above.

H295R cells were seeded 72 h before transfection at 30,000 cells/well in 96-well plates in DMEM/Ham's F-12 medium supplemented with 2 mM glutamine, 100 IU/mL penicillin, 100 µg/mL streptomycin, 10%

dextran charcoal-coated serum, 20 mM HEPES, a mixture of insulin/transferrin/selenium. Eighteen hours before transfection, cells were treated with 10^{-5} M metyrapone (Sigma-Aldrich), an inhibitor of the CYP11B1 enzyme. Cells were then cotransfected as described above with the *ZMYND8* intron 2-GIPR plasmid construct (100 ng), the hGR plasmid (100 ng), CRE-Luc (100 ng) and pRL-SV40 (Promega) (80 ng), as an internal reporter plasmid, in a serum-free OptiMEM® medium together with 10^{-5} M metyrapone. Six hours after tranfection, cells were pre-treated with 10^{-7} M dexamethasone (DEX), DEX and 10^{-5} M RU486, or ethanol in minimal medium containing 10^{-5} M metyrapone and 10% dextran charcoal-coated serum. Twenty-four hours later, cells were treated for 4 h with ethanol, 10^{-7} M GIP or 10^{-5} M H-89 in serum-free medium containing 10^{-4} M Ro 20-1724. Luciferase activities normalized to Renilla luciferase activities were expressed as a percentage of relative transcriptional activities compared with controls.

Tissue incubation

Fragments (~50 mm^3) of adrenocortical adenoma from patient #1 were weighed (~50 mg) and transferred to 6-well plates containing 2 ml of incubation medium (DMEM supplemented with 1% antibiotic-antimycotic solution; Gibco, Saint-Aubin, France). Incubation experiments were conducted in triplicate for 4 h in incubation medium with or without GIP and in the presence or absence of H89 (Sigma-Aldrich, Saint-Quentin Fallavier, France) at 37°C with 5% CO2. Incubation media were immediately frozen until hormone assay. Cortisol concentration in the supernatant was determined by RIA.

Immunohistochemistry

Adenoma tissue sections were deparaffinated and rehydrated. Sections were treated with a peroxidase inhibitor (Dako Corporation, Trappes, France). Tissue slices were incubated with antibody specific to GIPR (LSA3840; Lifespan Biosciences; 1:50) for 30 min at 23°C, and then with a streptavidin-biotin-peroxidase complex (Dako). Enzyme activity was revealed with diaminobenzidine. The tissue sections were counterstained with hematoxylin.

Supplemental Figure Legends

Supplemental Figure S1 Hormonal findings and adenoma characterization in patient #1

Panel A shows 24-hour profiles of plasma cortisol concentrations on 3 consecutive days. The patient took 3 mixed meals each day. On the third day (red curve), plasma cortisol was assayed in the clinostatic position. Plasma corticotropin was always undetectable. **Panel B** shows plasma cortisol concentrations measured during fasting and after a meal taken at 8 p.m. **Panel C** shows plasma cortisol concentrations measured after meals, with and without prior subcutaneous administration of 100 µg octreotide. **Panel D** shows a computed tomograph of the adrenal glands, revealing a 44-mm hypodense mass in the right adrenal gland (yellow arrow) and atrophy of the left adrenal gland (white arrow). **Panel E** shows cortisol secretion by adrenocortical adenoma fragments, with and without GIP and in the presence and absence of the PKA inhibitor H89. Data are mean values of triplicate determinations. T bars indicate standard deviation. Three asterisks indicate $P<0.001$. **Panel F** shows immunohistochemical staining of GIPR in the cytoplasm of adrenocortical adenoma cells. Nuclei (in blue) were stained with hematoxylin. Scale bars represent 50 µm.

Supplemental Figure S2 Adrenal expression of aberrant receptors in adrenal lesions of patients with GIP-dependent Cushing's syndrome or aldosteronoma.

Expression profiles of *ADRB1* encoding beta-adrenergic receptor type 1, *AGTR1* encoding angiotensin 2 receptor type 1, *AVPR1a* encoding vasopressin receptor type 1, *GnRHR* encoding gonadotropin-releasing hormone receptor, *HTR4* encoding serotonin receptor type 4, *LHCGR* encoding luteinizing hormone–chorionic gonadotropin receptor and *MC2R* encoding adrenocorticotropin receptor in adrenal tissue samples obtained by RT-qPCR and normalized to the β-actin housekeeping gene. The results are expressed as relative expression compared to mean expression level in the unaffected adrenal tissue samples, arbitrary set at 1. Expression in adrenal lesions more than 10-fold of expression in normal

adrenal tissue was considered significant. Data represent the mean of two independent experiments, each of which was performed in triplicate. The T bars indicate the standard error of the mean.

Supplemental Figure S3 Pyrosequencing of proximal *GIPR* promoter.

Panel A shows the analyzed sequence of *GIPR* promoter (chr19: 46,171,165-46,171,452), containing 10 CpGs (underlined) and several *cis*-acting regulatory elements. Of note, 3 CpGs are located close to functional Sp1/Sp3 binding motifs (bolded). **Panel B** shows absence of methylation in the proximal *GIPR* promoter in the normal adrenal tissue, and in adrenocortical adenoma samples (pooled) and bilateral macronodular adrenal hyperplasia samples (pooled) of patients with aberrant adrenal sensitivity to GIP.

Supplemental Figure S4 Global array-CGH profile of adrenal lesions of patients with GIP-dependent Cushing's syndrome or aldosteronoma.

CNVs identified in 5 adenoma samples and 11 hyperplasia samples are shown separately. Genomic gains are in blue, deletions in red.

Supplemental Figure S5 ***Expression of SNRPD2, QPCTL, FBXO46 and SIX5 genes in unaffected adrenals (control 1 and 2) and in 3 adrenal lesions with 19q13 duplication (from patients #1, #2 and #10).***

Expression profiles of these 4 genes in adrenal tissue samples were analyzed by RT-qPCR and normalized to the β-actin housekeeping gene. The results are expressed as relative expression compared to mean expression level in the unaffected adrenal tissue samples, arbitrary set at 1. Data represent the mean of one representative experiment performed in triplicate. The T bars indicate the standard error of the mean. Only expression in adrenal lesions more than 10-fold of expression in normal adrenal tissue was considered significant. Note that transcript levels of these 4 genes were very low in these samples (both in normal adrenal tissue and in adrenal lesions). I.e. in the lesion of the patient #10: *QPCTL* 3.1 +/- 0.9 molecules per µg of RNA, *FBXO46* 9.7 +/- 2.8 molecules per µg of RNA, *SIX5* 227 +/- 9.8 molecules per µg of

RNA and *SNRPD2* 168 +/- 38.4 molecules per µg of RNA. The modest and inconsistent differences in *SNRPD2, QPCTL, FBXO46* and *SIX5* expression in the 3 adrenal lesions with 19q10 duplication are in striking contrast with undisputable GIPR overexpression in these adrenal lesions: 574-fold in the adenoma of patient #1, 660-fold in the adenoma of patient #2 and 558-fold the hyperplasia of patient #10, as compared to normal adrenal tissue (Figure 1A).

Supplemental Figure S6 Structure of the *ZMYND8* intron 2-pGL4.26-Luc and *ZMYND8* intron 2-GIPR plasmid constructs used for luciferase assays.

The GRE sequence is indicated in red.

References

1. Chaumeil J, Augui S, Chow JC, Heard E. Combined immunofluorescence, RNA fluorescent in situ hybridization, and DNA fluorescent in situ hybridization to study chromatin changes, transcriptional activity, nuclear organization, and X-chromosome inactivation. Methods Mol Biol 2008;463:297-308.
2. Leggett RM, Clavijo BJ, Clissold L, Clark MD, Caccamo M. NextClip: an analysis and read preparation tool for Nextera Long Mate Pair libraries. Bioinformatics 2014;30:566-8.
3. Zeitouni B, Boeva V, Janoueix-Lerosey I, et al. SVDetect: a tool to identify genomic structural variations from paired-end and mate-pair sequencing data. Bioinformatics 2010;26:1895-6.
4. Boeva V, Lermine A, Barette C, Guillouf C, Barillot E. Nebula--a web-server for advanced ChIP-seq data analysis. Bioinformatics 2012;28:2517-9.

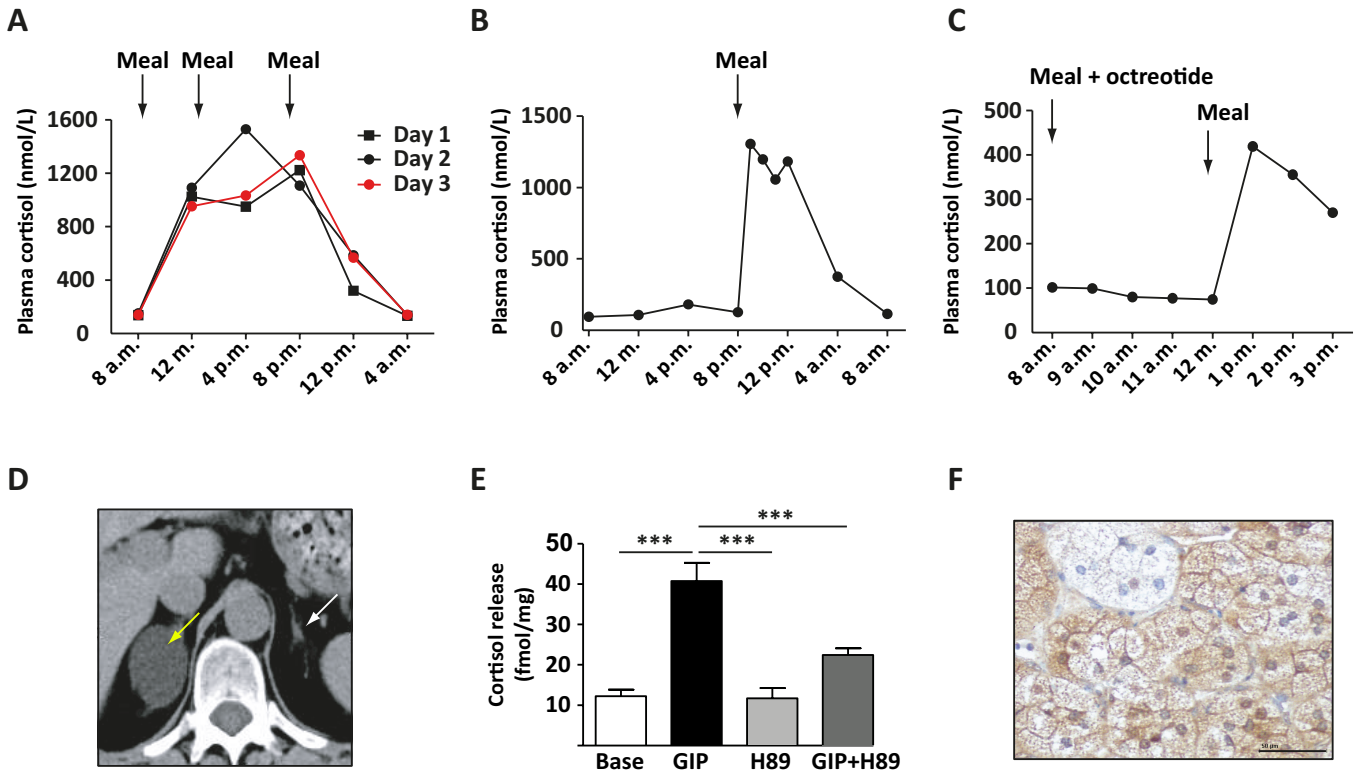

Supplemental Figure S1

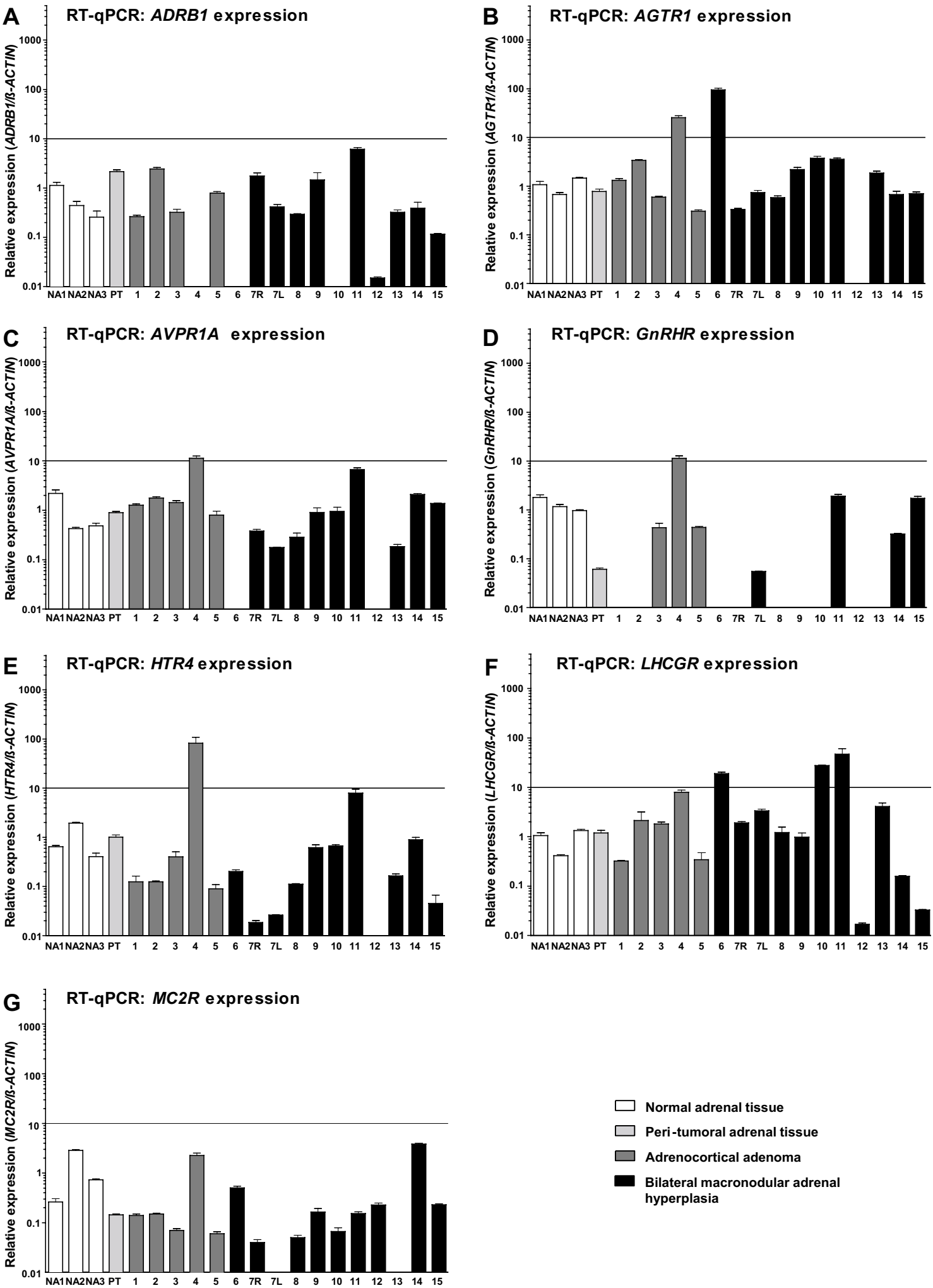

Supplemental Figure S2

A

TATTTGTGGGTGGGATAGTATGAGAGATTGTATATATTTGGTGTAGGGGTTTTTAGGACGATAAGGATAATTTAGTA
ATTGTTTTTTTTTATGATTTTGATGATTGTTTTTTGTTCGGTTTTTTGTTTTAGAGTTTT**TCGTTT**TCGTTTTTTGT
T**TCGTTT**TGGTT**TCGTTT**TTTTTTATTATTTCGGGTTGTTAGCGTTTGTTATTTTTTTTAGAGTCGAGATAAGGTAG
TTGGAGGTAGCGGTGGTAGGGGTTGTAGGAGTAAGTGATTAGGAGTAGGATTGGGG

B

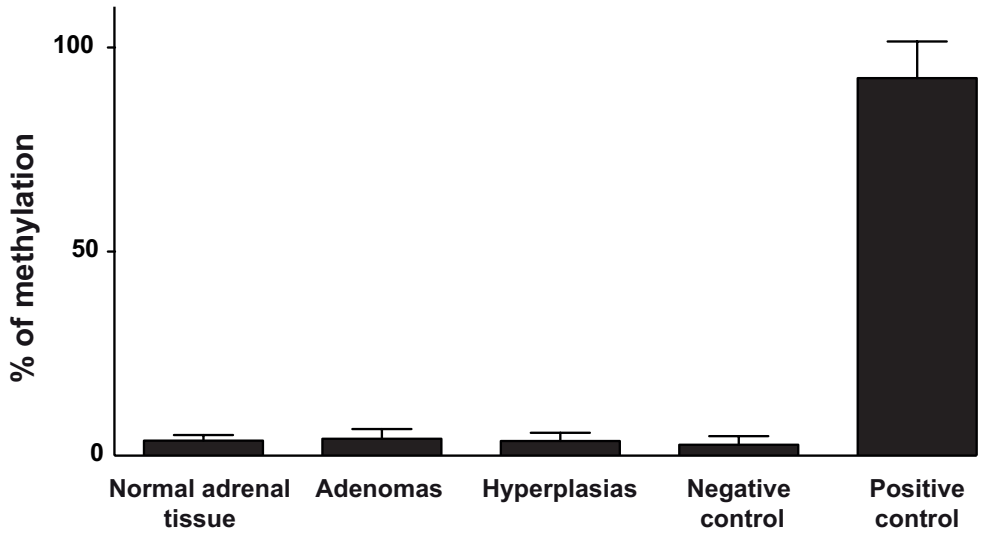

Supplemental Figure S3

Adrenocortical adenomas

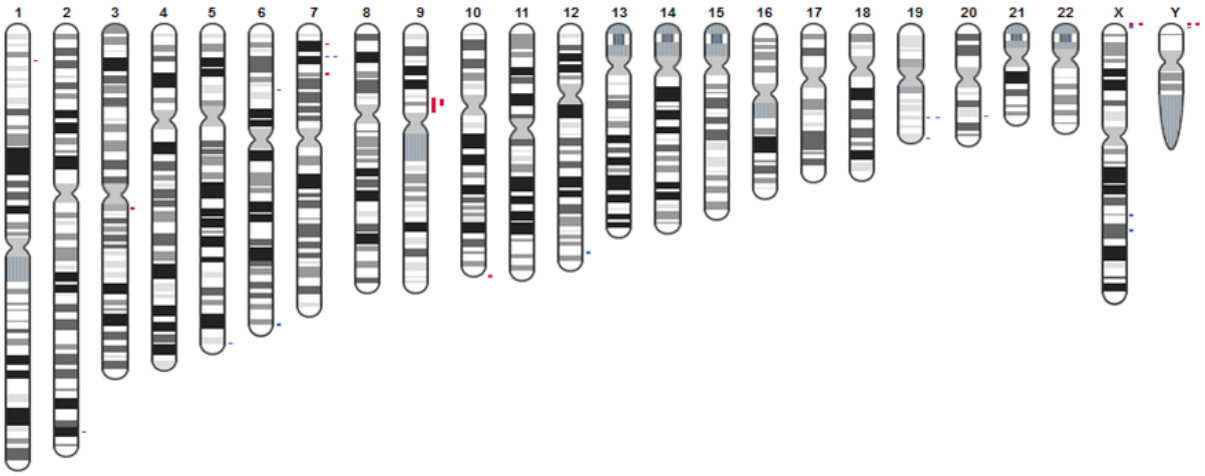

Bilateral macronodular adrenal hyperplasias

Supplemental Figure S4

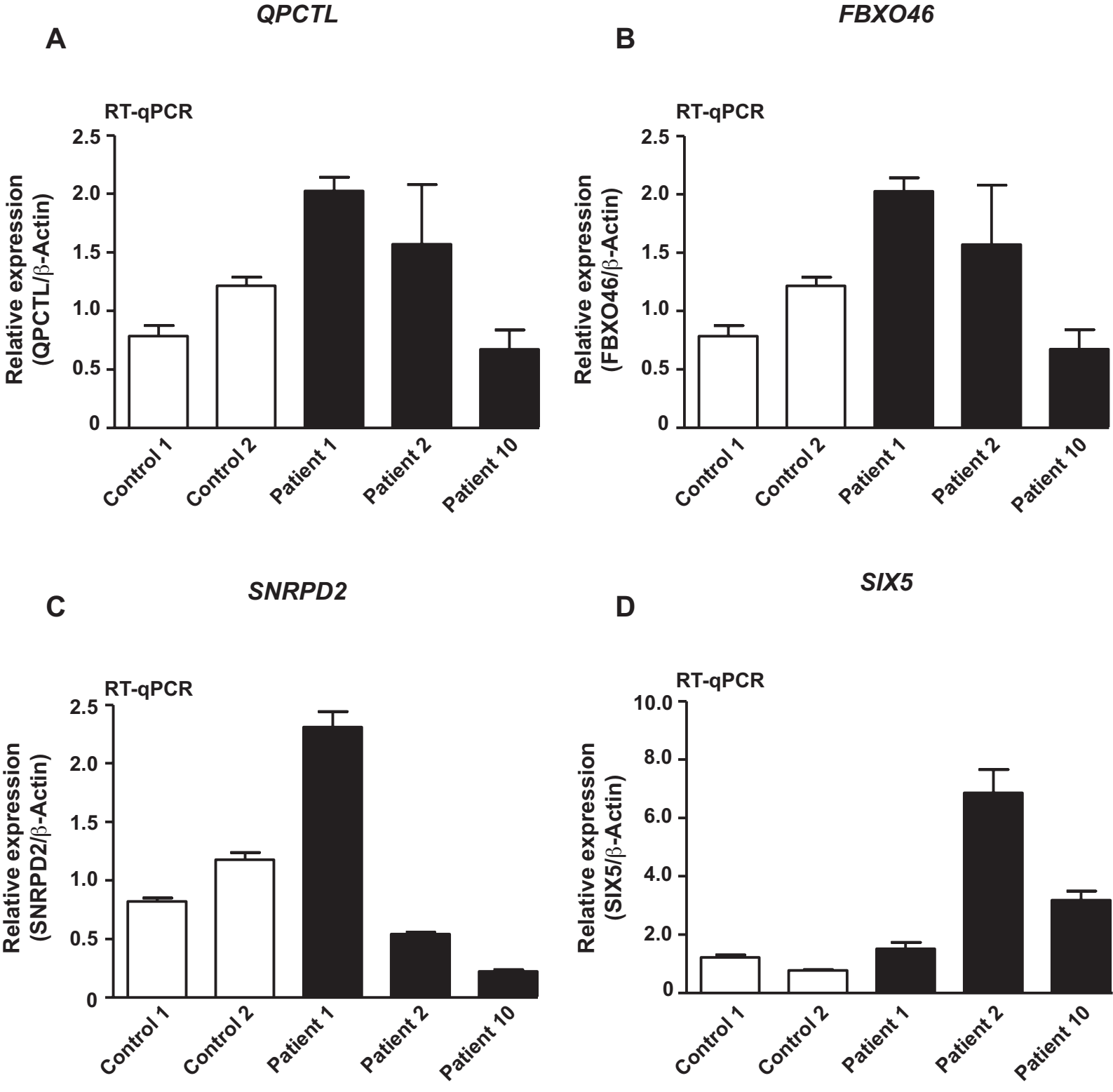

Supplemental Figure 5

A

AGCTTTGATTTCCTGGCTCAAGCAGTCCTCCCACTGCAGCCTCCCGAGTAGCTGGGACTACAGGTGTGCACTACC
ACCCCTGGCTAATGTTTATATTTTTTTGTAGAGATGAGGTTTCACTATGTTGCCCAGGCTGGTCTTGAACTCCTG
GGCTCAAGCGATCCTCCTGTCTTGGCCTCCCAAAGTGCTGGGATTGCTGGTGTGAGCCACCACTCCTGGGCCCAG
TTCTCCATTTAAAGTGAATAGTTTGATGGTTTTTAATATATTTTCACGGAGACCGGGTGTGGTGGCTGACGCCTG
TAATCCCAGCACTTTGGGAGGCCGAGGCGGGTGGATCACCTGAGGTCAGGAGTTCCGACCAGCCTGGCCAACATG
GTGAAACCCTGTCTCCACTAAAAATACAAAAAATTAGCTGAGTGTGGTGGCGTGTGCCTGTAATCCCAGCTACTC
AGCAGGCTGAGGCGGGAGAATTGCTTGAACGTGGGACGTGGAGGTTGCAGTGAGCCAAGATCGTGCCACTGTACT
CCAGCCCGGGTGACAGAGCAAGACTGCCTAAAATATATATATATATATATATATTTTTTTTTTTCACAGAGTTGT
GCAGCCAACAGCACAATCAGTTGTAGATTTTCATCACCCCCAATAAGAAACTTCATACTCATTAGCAGTCACTTC
CCATTCCCCCGTTACCCCTGTGCCTGGCAAGTACCAGTCTACTTTCTGTGCCTGTGGATTTGCTTATGCTAGACA
TTTCATATAAATGGAATCATACAGTATGTGACCTTTTGGTCTGAGTTCGTTCACTTAGAATAATGTTTTCAAGGC
TCATCCACATTCTTGTAGCATAGATCATC**AGTACAGACAGTTCC**TGACTTATAGTGGTGCGGAAGTGACAGTTCA
GTACAAACAGTACTTGGCATTTTGGATTTTTGATCTTTTCTCTGGCTAGCATCAGTATGAGACTCTCTTGGGGTG
CCAGGCACCTCCCAGTCAGCCACATGATCAC

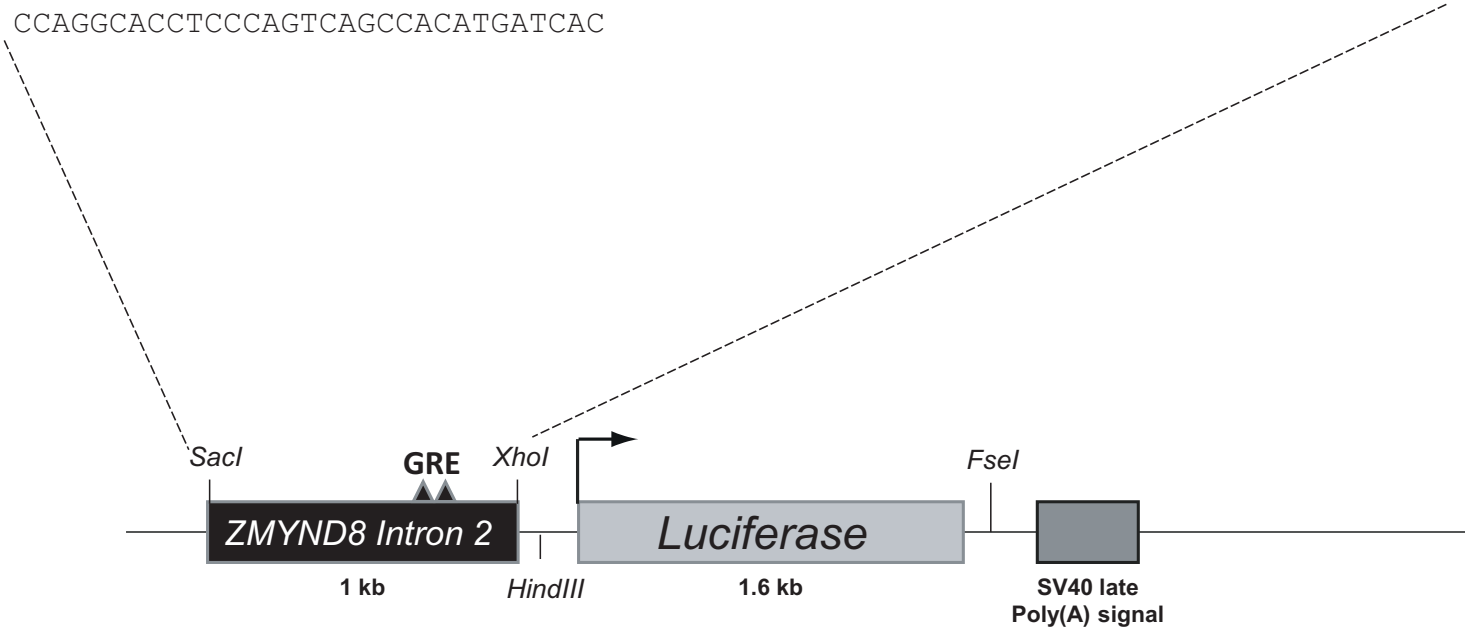

B

Supplemental Figure S6

Supplemental Table S1 Summary of CNVs detected by array-CGH in adrenal lesions of patients with GIP-dependent Cushing's syndrome or aldosteronoma.

Patient	Sample	CNV Nb	Size (min-max. kb)	Loss Nb	Gain Nb
1	Adenoma	4	67.44-100.44	1	3
2	Adenoma	2	191.91-338.88	0	2
3	Adenoma	6	10.34-404.09	3	3
4	Adenoma	8	9.21-8.457.29	6	2
5	Adenoma	6	12.89-4.587.30	2	4
6	Hyperplasia	26	10.84-120.591.17	13	13
7	Hyperplasia, right adrenal	9	10.84-120.604.32	4	5
	Hyperplasia, left adrenal	7	15.16-120.549.37	2	5
8	Hyperplasia	11	9.21-120.591.17	4	7
9	Hyperplasia	15	115.21-113.736.79	14	1
10	Hyperplasia	11	8.16-120.591.17	5	6
11	Hyperplasia	25	2.7-639.86	2	23
12	Hyperplasia	3	481.55-98.813.47	3	0
13	Hyperplasia	1	120.575.77	1	0
14	Hyperplasia	1	30.80	0	1
15	Hyperplasia	15	287.33-108.907.18	13	2

The number of CNVs varied from 1 to 26 per sample. In adrenocortical adenomas very few CNVs were detected, located mostly on instable regions of the genome. In contrast, primary bilateral macronodular adrenal hyperplasias showed a higher number of extensive chromosomal imbalances.

Supplemental Table S2 Detailed description of CNVs detected by array-CGH in adrenal lesions of patients with GIP-dependent Cushing's syndrome or aldosteronoma.

Patient	Sample	Gains		Losses		Size (kb)
		Chromosomal region	start-stop (hg19)	Chromosomal region	start-stop (hg19)	
1	Adenoma			7p21.3	8.693.710-8.764.517	70.81
		12q24.31	123.969.506-124.043.818			74.31
		19q13.32	46.167.704-46.268.140			100.44
		20q13.12	45.952.305-46.019.749			67.44
2	Adenoma	19q13.32	46.149.049-46.340.961			191.91
		19q13.43	57.483.767-57.822.649			338.88
3	Adenoma	5q35.2	176.041.560-176.051.896			10.34
		6p21.31	35.203.234-35.227.959			24.73
		7p21.2	16.240.510-16.255.671			15.16
				10q26.3	134.391.564-134.795.657	404.09
				Xp22.33	81.548-92.387	10.84
				Yp11.32	31.548-42.387	10.84
4	Adenoma			1p36.13	17.594.882-17.621.864	26.98
				3q11.2	96.287.058-96.316.860	29.80
				7p15.2	26.137.319-26.175.778	38.46
				9p13.1p11.2	38.755.124-47.212.417	8.457.29
				Xp22.33	81.548-92.387	10.84
		Xq22.2	102.816.308-102.825.521			9.21
		Xq23	111.711.991-111.734.734			22.74
				Yp11.32	31.548-42.387	10.84
5	Adenoma			2q36.3	228.243.887-228.256.777	12.89
		6q26	163.920.296-163.942.106			21.81
		7p21.2	16.240.510-16.255.671			15.16
				9p13.1p11.2	39.072.211-43.659.512	4.587.30
		Xp22.33	880.956-943.314			62.36
		Yp11.32	830.956-893.314			62.36
6	Hyperplasia			1p36.33p11.2	759.762-121.350.930	120.591.17
		1p32.3	55.054.621-55.199.256			144.64
				1q21.2	149.041.933-149.581.094	539.16
		1q21.3	152.556.449-152.586.281			29.83
		1q24.2	169.216.643-169.241.333			24.69
				2p25.3	17.019-84.728	67.71
		2p25.3p24.3	469.914-15.051.058			14.581.14
				2p25.1	11.426.657-11.938.779	512.12
				2p24.3	15.893.132-16.375.214	482.08
				2p24.2	16.952.523-17.055.306	102.78
				2p24.1p12	19.924.907-78.633.918	58.709.01
		2p23.3	25.045.201-25.122.236			77.04
		2p23.3p23.2	26.472.591-28.476.960			2.004.37
				2p22.3	35.967.990-35.990.844	22.85
		2p22.2	37.958.541-38.002.391			43.85
		2p13.3	70.866.336-70.992.030			125.69
		2p12	76.351.666-76.437.349			85.68
				2q36.3	228.243.887-228.256.777	12.89
				5p15.33p13.3	26.142-29.160.570	29.134.43
		6q26	163.920.296-163.950.870			30.57
		7p21.2	16.240.510-16.255.671			15.16
		10q24.33	105.191.824-105.222.032			30.21
				17q11.1q25.2	25.375.449-75.163.576	49.788.13
				22q11.1q13.33	16.133.474-51.170.223	35.036.75

				Xp22.33	81.548-92.387	10.84
		Xp22.33	928.806-940.732			11.93
7	Hyperplasia, right adrenal			1p36.33p11.2	746.608-121.350.930	120.604.32
		1p31.1	83.616.238-83.866.100			249.86
		1p22.3	88.079.298-88.127.475			48.18
		5p15.33p11	42.109-46.115.086			46.072.98
		6q26	163.920.296-163.942.106			21.81
		7p21.2	16.240.510-16.255.671			15.16
				13q21.1	58.157.668-58.194.488	36.82
				Xp22.33	81.548-92.387	10.84
				Yp11.32	31.548-42.387	10.84
	Hyperplasia, left adrenal			1p36.33p11.2	801.556-121.350.930	120.549.37
		1p12p11.2	120.529.670-120.903.682			374.01
		1q21.1q44	145.264.630-249.212.668			103.948.04
		3p21.31	47.234.542-47.257.077			22.54
		6q26	163.920.296-163.950.870			30.57
		7p21.2	16.240.510-16.255.671			15.16
				13q21.1	58.157.668-58.194.488	36.82
8	Hyperplasia			1p36.33p11.2	759.762-121.350.930	120.591.17
		1p35.3	29.641.035-29.653.134			12.10
		1p34.2	43.731.986-43.748.554			16.57
		5p15.33p11	42.109-46.115.086			46.072.98
		6p21.31	35.203.234-35.227.959			24.73
				8p21.2	27.319.797-27.349.027	29.23
				16q11.2q24.3	46.587.892-90.118.285	43.530.39
				Xp22.33	81.548-92.387	10.84
		Xp22.33	898.287-908.212			9.93
		Xq22.2	102.816.308-102.825.521			9.21
		Xq23	111.711.991-111.734.734			22.74
9	Hyperplasia			1p36.33p13.2	746.608-114.483.398	113.736.79
		1p13.3	107.755.754-108.164.476			408.72
				1p13.3	108.926.313-109.247.547	321.23
				1p13.3p13.2	111.535.290-112.366.718	831.43
				1p13.1	116.919.588-117.034.794	115.21
				1p12	118.158.972-120.176.982	2.018.01
				2q24.2	162.770.039-163.144.683	374.64
				6p22.1	27.526.618-28.297.558	770.94
				9p24.3p11.2	220.253-43.836.428	43.616.18
				10p15.1p11.1	6.578.408-38.134.373	31.555.97
				10q26.11q26.12	121.199.229-121.983.218	783.99
				13q14.11q34	42.259.224-115.105.297	72.846.07
				15q13.3q26.1	33.009.424-90.345.391	57.335.97
				18q21.2	51.431.756-51.715.252	283.50
				Xp11.21	56.992.484-57.704.961	712.48
10	Hyperplasia			1p36.33p11.2	759.762-121.350.930	120.591.17
		1p32.3	55.085.200-55.093.357			8.16
		1p12p11.2	120.529.670-120.614.056			84.39
		1q21.1q44	145.264.630-249.212.668			103.948.04
		7p21.2	16.240.510-16.255.671			15.16
				7q31.32	123.772.959-123.786.416	13.46
				11p12	40.041.124-40.107.104	65.98
		15q26.2	97.018.166-97.043.083			24.92
				16q12.2	55.799.203-55.822.392	23.19
		19q12q13.43	31.965.977-59.095.418			27.129.44
				Xq22.2	102.816.308-102.825.521	9.21
11	Hyperplasia	1p36.32	3.832.693-3.844.918			12.23
		1p36.22	9.904.660-9.975.048			70.39
		1p34.2	43.731.986-43.748.554			16.57

		1p13.3	110.281.079-110.314.306			33.23
		2q31.1	169.907.405-169.918.656			11.25
		3p22.1	41.879.402-41.894.198			14.80
		5q35.2	176.041.560-176.051.896			10.34
		6p21.31	35.203.234-35.227.959			24.73
		6q26	163.920.296-163.942.106			21.81
		7p21.2	16.240.510-16.255.671			15.16
		10q21.2	61.320.179-61.362.005			41.83
		11p15.5	1.743.904-2.383.763			639.86
		11q13.1	64.107.266-64.208.595			101.33
		11q13.2	66.093.417-66.108.523			15.11
		14q11.2	20.732.596-20.760.405			27.81
		14q32.32	103.528.110-103.586.240			58.13
		15q23	68.065.053-68.113.794			48.74
		19p13.2	11.296.314-11.321.918			25.60
				19p13.11	19.351.556-19.612.665	261.11
		19q13.12	36.357.708-36.370.533			12.83
		19q13.33	50.973.797-51.387.349			413.55
				Xp22.33	81.548-92.387	10.84
		Xp22.33	556.373-561.307			4.93
		Xp22.33	578.537-590.689			12.15
		Xq28	151.119.742-151.122.438			2.70
12	Hyperplasia			1p36.33p21.3	746.608-99.560.081	98.813.47
				11p15.4	9.181.761-9.663.311	481.55
				15q11.1q12	20.102.541-26.309.444	6.206.90
13	Hyperplasia			1p36.33 - p11.2	746.608-121.322.377	120.575.77
14	Hyperplasia	6q26	163.911.310-163.942.106			30.80
15	Hyperplasia	2p22.1	39.270.599-39.622.894			352.30
				6p25.3p11.2	389.423-58.686.125	58.296.70
				6q11.1q27	61.982.931-170.890.108	108.907.18
				11p15.5p11.12	210.300-51.511.461	51.301.16
				11q11q25	55.028.487-134.927.114	79.898.63
				14q11.2q32.33	19.376.762-107.278.770	87.902.01
				18p11.32p11.21	118.760-14.966.054	14.847.29
				18q11.1q23	18.529.851-78.010.032	59.480.18
				22q11.1q13.33	16.133.474-51.178.264	35.044.79
				Xp22.33	61.091-2.052.995	1.991.90
				Xp22.33p11.21	2.373.908-58.051.765	55.677.86
				Xq11.1q28	61.931.689-155.190.083	93.258.39
				Yp11.32p11.2	11.091-3.714.007	3.702.92
		Yp11.32	2.016.581-2.303.907			287.33
				Yq11.23q12	28.754.210-59.310.245	30.556.04

Supplemental Table S3 Recurrent CNVs detected by array-CGH in adrenal lesions of patients with GIP-dependent Cushing's syndrome or aldosteronoma.

Adrenal histology	Patient No	Chromosomal region (start-stop. hg19)	Size (kb)	CNV type
Hyperplasia	6,7,8,9,10,12,13	chr1:801.556-99.560.081	98.813.53	loss
Hyperplasia	8,11	chr1:43.731.986-43.748.554	16.57	gain
Hyperplasia	6,10	chr1:55.085.200-55.093.357	8.16	gain
Hyperplasia	6,7,8,10,13	chr1:116.919.588-117.034.794	115.21	loss
Hyperplasia	6,7,8,10,13	chr1:118.158.972-120.176.982	2.018.01	loss
Hyperplasia	7,8	chr5:42.109-46.115.086	46.073.98	gain
Hyperplasia	9,15	chr6:27.526.618-28.297.558	770.94	loss
Hyperplasia	8,11	chr6:35.203.234-35.227.959	24.73	gain
Hyperplasia	6,7,11,14	chr6:163.920.296-163.942.106	21.81	gain
Adenoma / Hyperplasia	3,5,6,7,10,11	chr7:16.240.510-16.255.671	15.16	gain
Adenoma	4,5	chr9:39.072.211-43.659.512	4.587.30	loss
Hyperplasia	12,15	chr11:9.181.761-9.663.311	481.55	loss
Hyperplasia	10,15	chr11:40.041.124-40.107.104	65.98	loss
Hyperplasia	7,9	chr13:58.157.668- 58.194.488	36.82	loss
Hyperplasia	8,10	chr16:55.799.203-55.822.392	23.2	loss
Hyperplasia	9,15	chr18:51.431.756-51.715.252	283.50	loss
Adenoma	1,2	chr19:46.167.704-46.268.140	100.44	gain
Hyperplasia	6,15	chr22:16.133.474- 51.170.223	35.036.75	loss
Adenoma / Hyperplasia	3,4,6,7,8,11,15	chrX:81.548-92.387	10.84	loss
Hyperplasia	10,15	chrX:102.816.308-102.825.521	9.21	loss
Adenoma / Hyperplasia	3,4,7,15	chrY:31.548-42.387	10.84	loss

A total of 16 recurrent DNA variations in primary bilateral macronodular adrenal hyperplasias, 2 recurrent DNA variations in adrenocortical adenomas and 3 recurrent DNA variations common to both adenomas and hyperplasias were detected.

Table S4 Primer sequences used for quantitative RT-PCR, genomic PCR, pyrosequencing and the GIPR antibody used for immunohistochemistry.

Primer sequences used for the cloning of ZMYND8 intron 2

Name	*Sense primer*	*Antisense primer*
ZMYND8 intron 2	5'-GCGTGAGCTCAGCTTTGATTTCCTGGCTCA-3'	5'-CGCCCTCGAGCGTGATCATGTGGCTGACTGG-3'

Primer sequences used for quantitative RT-qPCR

Name	*Accession number*	*Amplicon size (bp)*	*Sense primer*	*Antisense primer*
ADRB1	NM_000684.2	79	5'-GCCCACAATCCTCGTCTGAA-3'	5'-CCCTTCCCAAACTTTCCTTTTT-3'
AGTR1	NM_000685.4	99	5'-GCTTCAGCCAGCGTCAGTTT-3'	5'-GGGACTTCATTGGGTGAACAA-3'
AVPR1A	NM_000706.4	80	5'-CTTCCCGTCGCAAACATAGG-3'	5'-CGCTCGTGACTTAAAGAGCTATCTC-3'
β-ACTIN	NM_001101.3	150	5'-GCATGGGTCAGAAGGATTCCT-3'	5'-ACACGCAGCTCATTGTAGAAGG-3'
FBXO46	NM_001080469.1	150	5'-CCTTTGCCTCGCTTTTGACA-3'	5'-GGA AGG AAA AAC CCA GAA A-3'
GIPR	NM_000164.3	99	5'-TGCCCTTCTGGAGATGACAAC-3'	5'-TTCTCGCTTCCCTTCATAACCA-3'
GnRHR	NM_000406.2	102	5'-CACGGGTCCTTCATCAGG-3'	5'-GCAAATGCAACCGTCATTTT-3'
HTR4	NM_001040169.2	81	5'-AGTCGGCAGACCAGCATAGC-3'	5'-AAGCAACCCATGATGATGCA-3'
LHCGR	NM_000233.3	99	5'-CCCTGGAAAGGATAGAAGCTAATG-3'	5'-GCTCCGGGCTCAATGTATCTC-3'
MC2R	NM_000529.2	197	5'-GGACCGCTACATCACCATCT-3'	5'-AGGCACAGGATGAAGACCAG-3'
QPCTL	NM_017659.3	79	5'-GGATGACAGCCAGAGGAATAAGAA-3'	5'-GTATTTGGTCCCTGCAAACCTTT-3'
SIX5	NM_175875.4	123	5'-CCCGTTACCTTCTGCGTTGT-3'	5'-CGTCTGTCTGTGATTCTCCCTTT-3'
SNRPD2	NM_004597.5	99	5'-TCATCAACTGCCGCAACAAT-3'	5'-TCAGTCCACATCTCCTTCACGTT-3'
ZMYND8	NM_183047.3	120	5'-AGGTCGATGCCCGATTCTTT-3'	5'-GCACTGTTGAAGATGCTCTTAGTCTT-3'

Primer sequences used for PCR amplification of GIPR promoter after sodium bisulfite treatment

Name	*Sense primer*	*Antisense primer*
GIPR Promoter	5'-TATTTGTGGGTGGGATAGTATGAGA-3'	5'-CCCCAATCCTACTCCTAATCACTTA-3'

Primer sequences used for pyrosequencing of GIPR promoter after sodium bisulfite treatment

Name	*Sequence*	*Name*	*Sequence*
GIPR Promoter #1	5'-TATATTTGGTGTAGG-3'	*GIPR* Promoter #2	5'-TTATGATTTTGATGA-3'
GIPR Promoter #3	5'-TTGTTTTAGAGTTTT-3'	*GIPR* Promoter #4	5'-GTTTTTTTTTATTAT-3'